리그닌 함유 셀룰로오스 나노섬유로 강화된 폴리락틴산
나노복합재의 제조 및 분석

Haibo Sun, Xuan Wang, and Liping Zhang[†]

MOE Engineering Research Center of Forestry Biomass Materials and Bioenergy, Beijing Forestry University
(2013년 12월 23일 접수, 2014년 2월 15일 수정, 2014년 2월 18일 채택)

Preparation and Characterization of Poly(lactic acid) Nanocomposites Reinforced with Lignin-containing Cellulose Nanofibrils

Haibo Sun, Xuan Wang, and Liping Zhang[†]

MOE Engineering Research Center of Forestry Biomass Materials and Bioenergy, Beijing Forestry University,
No.35 Qinghua East Road, Beijing 100083, China
(Received December 23, 2013; Revised February 15, 2014; Accepted February 18, 2014)

Abstract: A chemo-mechanical method was used to prepare lignin-containing cellulose nanofibrils(L-CNF) from unbleached woodpulps dispersed uniformly in an organic solvent. L-CNF/PLA composites were obtained by solvent casting method. The effects of L-CNF concentration on the composite performances were characterized by tensile test machine, contact angle machine, scanning electron microscope (SEM), and Fourier transform infrared spectroscopy (FTIR). The tensile test results indicated that the tensile strength and elongation-at-break increased by 50.6% and 31.8% compared with pure PLA. The contact angle of PLA composites decreased from 79.3° to 68.9°. The FTIR analysis successfully showed that L-CNF had formed intermolecular hydrogen bonding with PLA matrix.

Keywords: lignin-containing cellulose nanofibrils, poly(lactic acid), nanocomposites, reinforcement.

Introduction

Nowadays, popular concepts such as 'sustainable development' and 'quality of life' have considerable impact on the activities in the protection of environment, in order to help reduce environmental pollution caused by petroleum-based products, decrease the dependence on nonrenewable resources, people have developed biobased material with controlled properties.[1-4]

Poly(lactic acid) (PLA) is linear aliphatic thermoplastic polyester that can be derived from the fermentation of renewable resources such as corn starch.[5] Using such bio-based materials can help maintain the balance of carbon in nature. Comparing with traditional plastics, PLA has a lot of good properties, including biodegradability, biocompatibility and good mechanical properties. However, with a glass transition temperature ranging from 55 to 65 centigrade degree, PLA is too stiff and brittle for room temperature application.[6,7] The

low impact strength and low ability in resisting thermal deformation, which limiting the extensive application of pure PLA.[8]

Lignin is an abundant non-toxic amorphous natural polymer and an inexpensive by-product of the paper industry. The global production of lignin in pulp mills industry amounts had approached the half of the total production of industrial plastics.[9] Lignin structure is chemically complex and the main monomer units are 2-methoxy-4-propylphenol in soft wood and a mixture of guajacol and 1,5-dimethoxy-4-propylphenol in hardwood.[10] Due to these functional groups, the lignin micromolecule gets a high polarity. Because of these characteristic, especially its biodegradability, lignin is an extremely promising material as a chemical component in polymer blends or as a filler in the field of organic filler.

Cellulose, the world's most abundant, natural, renewable and biodegradable polymer,[11] can be found in many bio-resources. Cellulose is a polydisperse linear polymer of poly-(1,4)-*D*-glucose residues. The monomers are linked together by condensation, such that the sugar rings are joined by glycosidic oxygen bridges. Cellulose consists of crystalline phases and amorphous phases at a nanometer level, which are bonded by

intra- and inter-molecular hydrogen bonds and vander Waals forces that maintain the self-assembled macromolecular structure and the fibril morphology. Cellulose nanofibrils can be obtained by chemical, physical biological processs.[12-14] The most popular mechanical process to disintegrate the nature cellulose microfibril assembly is through high-pressure homogenization of a cellulose-solvent suspension. With multiple passes at a high pressure, microfibrillated cellulose can be produced with average widths well below 100 nm and is increasingly referred to as cellulose nanofiber, nanofibril, and nanocellulose.[15] Geometrical characteristics of cellulose nanofibrils depend on both the origin of cellulose and the processing conditions such as time, temperature and purity of materials.

Cellulose nanofibrils have already act as reinforcing elements because of cellulose nanofibrils consist of slender parallelepiped rods with lateral dimension at the nanometer level, high aspect ratio, large surface areas and renewable character. Cellulose nanofibrils have been mainly employed as filler in several kinds of polymeric matrix from aqueous suspension.[16,17]

A lot of papers have studied about lignin and cellulose as polymer blending filler. Cellulose and lignin as polymer fiiler can improve the properties of composites such as mechanical properties, hydrophilicity property and degradation property apparently, which could be reflected by Figure 1 in our study. The hydrogen bond interaction could explain this phenomenon. However, blending lignin and cellulose with polymers has got few research reports. In order to use this two nature and

renewable resources enough, there is a great step for us to take.

In the present study, we report the use of unbleached kraft pulps to get L-CNF, using a new method to make the L-CNF disperse homogeneously in an organic solvent in preparation for composite formation. In addition, a solution-casting method, which can avoid the degradation, was used to produce the nanocomposites. The lignin existing can improve the compatibility between cellulose nanofibrils and PLA matrix to some extent. So, the properties of the obtained L-CNF/PLA composites were improved compared with the pure PLA.

Besides the usage of modified PLA in packaging, the nanocomposites can be a potential tissue engineering implant in the clinical application because of the better biocompatibility. The abundant exposed hydroxyl (-OH) groups offered the nanocomposites a good hydrophilicity property and contribute to their biodegradability. The degradation rate also can be controlled by adding different content of L-CNF.

Experimental

Materials. Unbleached Kraft wood pulp board (lignin content: 5%, sulfate cooking) was purchased from a pulp and paper mill in Inner Mongolia, China. Poly(lactic acid) (PLA, Mw=100000 purchased from Shanghai Yisheng industry Ltd.) was used as the matrix. N,N-Dimethylacetamide (DMAc) and sulfuric acid (98%) were purchased from Shantou Xilong Chemical Plant and Beijing Chemical Plant, respectively.

Preparation of Nanocomposites. Preparation of Suspension of Lignin-containing Cellulose Nanofibrils in Organic Solvent: After the pretreatment of the Kraft pulp board in diluted sulfuric acid (15%) at a constant mixing speed of 150 rpm for 4 h at 85 °C (at a solid to liquid ratio of 1: 20 g/g), the suspension was vacuum filtered, and the cake was washed first with deionized water to remove the H^+ and SO_4^{2-}, then washed with DMAc to remove the water in it. After that, the cake was immersed into DMAc, and the pretreated lignin-containing cellulose was suspended in the DMAc, which was then homogenized at a high pressure of 100 MPa for 10 cycles (GEA Niro Soavi, Italy). Through the combination of pretreatment and homogenization, the L-CNF became well dispersed in DMAc.

Preparation of Neat PLA: The solvent casting and evaporation method was used to prepare the composite samples. A 16 wt% solution of PLA in DMAc was prepared by stirring the solution in a water bath at 70 °C. The PLA was scraped with a scraper on glass and then dried on an electric heating board
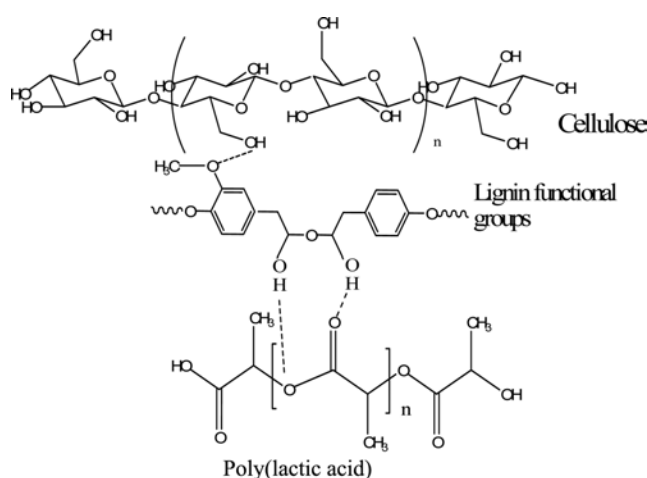
Figure 1. Hydrogen bonding interactions between the reactive functional groups in lignin-containing cellulose and the carbonyl groups of PLA.

at 80 °C. After that, the obtained PLA was placed under vacuum condition at 40 °C for 24 h to ensure the solvent had completely evaporated.

Preparation of L-CNF/PLA Composite: First, the L-CNF was dispersed in DMAc to form a suspension. Then, PLA was added into the suspension at 70 °C with agitation in an ultrasonic bath for 2 h (KQ5200DB, China). The composited was scraped with a scraper on glass and then dried on an electric heating board at 80 °C. The lignin-containing cellulose nanofibrils content in PLA nanocomposite was 0 to 5 wt% (based on polymer content). After that, the obtained composites were placed under vacuum condition at 40 °C for 24 h to ensure the solvent had completely evaporated.

Testing and Characterization. Mechanical Tests: In order to determine the tensile strength, the size of the samples used was 100 mm×15 mm. A tensile testing machine (DCP-KZ300) was used to measure the tensile strength at the point of breakage of each composite. Testing was conducted at a crosshead speed of 20 mm/min. Five measurements were made for each specimen, and the data averaged to obtain a mean value.

Transmission Electron Microscope (TEM): The L-CNF suspensions were deposited onto glow-discharged carbon-coated transmission electron microscopy grids and negatively stained with 2% phosphotungstic acid. Images of the specimens were examined with a HITACHI H-600 transmission electron microscope at an acceleration voltage of 80 kV.

Scanning Electron Microscope (SEM): The fracture surfaces of pure PLA, PLA with different content of L-CNF composites were studied with an S-3000 scanning electron microscopy under an accelerating voltage of 15 kV. All samples were broken to expose the internal structure for SEM studies before the examination, and the entire surface were sputtered with gold.

Hydrophilicity of Nanocomposites: The contact angle θ can be used to measure the degree of hydrophilicity. The water contact angle (WCA) was determined by using a HARKE-SPCA contact angle analyser (Beijing Hake, Ltd) for the air side. To determine the effect of L-CNF on WCA. The composites were air dried for 24 h. The surface energy W_A can be calculated by following eq. (1).

$$W_A = \gamma_w \cdot (1 + \cos\theta) \tag{1}$$

Where the surface tension γ_w is 7.28×10^{-2} N/m.

X-Ray Diffraction. The degree of L-CNF, pure PLA, L-CNF/PLA composites were tested with an X-ray diffraction instrument (Shimadzu XRD-6000, Japan) with Cu, Kcr radial, Ni filter, X=0.154 nm, scan range: 2θ=5-40°, and scan step:=0.2°/3 s. The degree of crystallinity of samples were calculated according to the eq. (2).

$$I_c\ (\%) = \frac{I_{(\text{Crys}+\text{am})} - I_{\text{am}}}{I_{\text{am}}} \times 100 \tag{2}$$

where $I_{(\text{Crys}+\text{am})}$ is the peak intensity (counts per second) at roughly 22.8° for the crystalline and amorphous parts and I_{am} is the peak intensity at roughly 18°, representing the amorphous part of the CNF.

FTIR Characterization. FTIR Spectra of the lignin-containing cellulose was obtained with dried powdered samples on a Tensor 27 (Bruker, Germany) device in the range of 4500-500 cm⁻¹. Pallets were prepared from the mixtures of the samples and KBr (1:100, w/w). 32 scans were accumulated at a resolution of 2 cm⁻¹.

Results and Discussion

Structure of L-CNF. Figure 2 shows the transmission electron microscopy obtained for L-CNF resulting from sulphuric acid hydrolysis of unbleached kraft wood pulps. The length and the width of L-CNF were measured from the TEM image and a large number of nanofibers had been gotten by acid hydrolysis. The dimension of the L-CNF were about 50 nm in width and several micrometers in length.

Mechanical Properties of Nanocomposites. The result of mechanical test was present in Figure 3, it showed that the
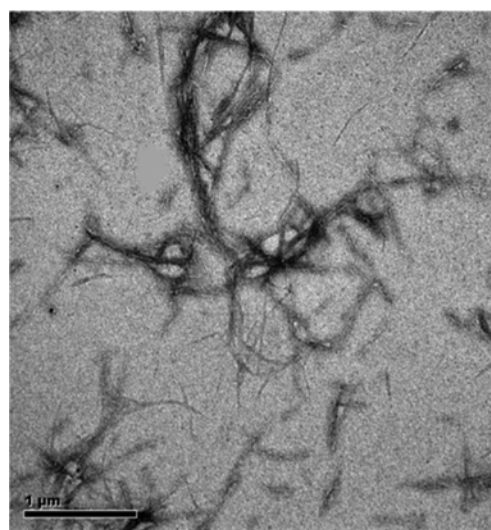
Figure 2. Structure of the L-CNF analyzed with TEM.

effect of CNF and L-CNF on the tensile strength and elongation at break of PLA composites. After adding the cellulose nanofibrils (CNF) to the PLA matrix, its mechanical properties decreased compared with pure PLA. However, the L-CNF was added to the PLA matrix, the composites showed significant improvements in tensile strength and elongation.

The reason might be explained that the interfacial bonding between cellulose nanofibrils and PLA matrix is poor, and the existence of the cellulose nanofibrils, as an obstruction, separates the molecular chains of PLA, which makes the distance among the molecules larger and the force among the molecular chains of PLA weaker. The interaction between PLA and cellulose nanofibrils was too weak to counteract the loading. However, the existence of lignin made it easy for the compatibility of cellulose nanofibrils and PLA. The presence of lignin had improved adhension between fiber and matrix, sim-

Figure 3. Tensile strength and elongation of different kinds of composites.

Figure 4. Different L-CNF contents on mechanical properties of the composites.

ilar phenomenon was found by Kang *et al.*[18] As a result, the mechanical propertied of PLA composites could be improved by adding appropriate content of L-CNF.

The tensile strength and elongation-at-break of PLA composites with different content of L-CNF were depicted in Figure 4. Both the tensile and elongation characterizations were enhanced with adding L-CNF in PLA composites. Compared with the pure PLA, The index of the composites tensile strength firstly increased with the addition of L-CNF, reached its peak value when the content of L-CNF was 3% and then decreased with further increase of L-CNF. A similar variation trend was observed from the elongation of L-CNF/PLA composites. The elongation-at-break increased with the addition of L-CNF and reached its peak value with the content of nanofibris at 3%. These trends can be explained as follows. The nano effect endows nanofibrils with a lot of special characters such as fine mechanical properties, the high aspect ratio of the nanofibrils and their web structures contribute greatly to the strength improvement. However the increased aggregation among nanofibrils could weaken the tensile strength and elongation-at-break of the composites. It could be explained that why both of the tensile strength and elongation at break decreased when the content of L-CNF was more than an optimum concentration. The tensile strength increased from 15 MPa of pure PLA to 22.6 MPa of the optimal L-CNF/ PLA composites.

Hydrophilic Properties of Nanocomposite. The hydrophilicity of a polymer material can be evaluated by its contact angle (θ) with water. In general, composite surface hydrophilicity is higher when its contact angle is smaller. From Figure 5(a), it can be seen that the L-CNF could improve the hydrophilicity of PLA. However, by addition the same content (2%) of CNF and L-CNF, the CNF/PLA composite had better hydrophilicity property comparing with L-CNF/PLA composite, which can be explained that lignin is less hydrophilic than cellulose.

It is also known that the water contact angle correlates with surface roughness because of the solid-liquid-gas interfaces associated with a macroporous surface.[19] The contact angle and surface energy of pure PLA and PLA composites with different content of L-CNF are showed in Figure 5(b). Comparing to the pure PLA, the contact angle of composites dropped gradually from 79.3° to 68.9°, the surface energies were increased from 86.31 to 99.12 mN/m², which showed the difference compared with the characteristic of mechanical strength, the distribution of L-CNF in the matrix could sig-
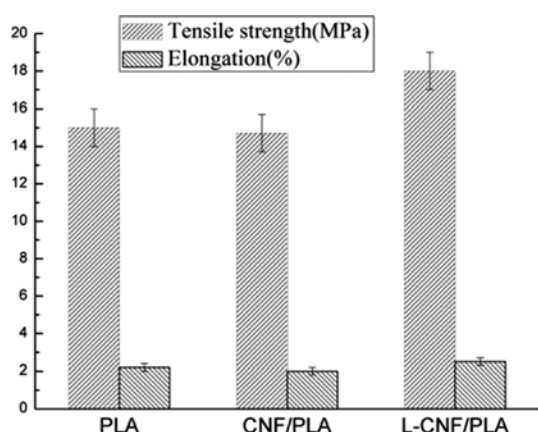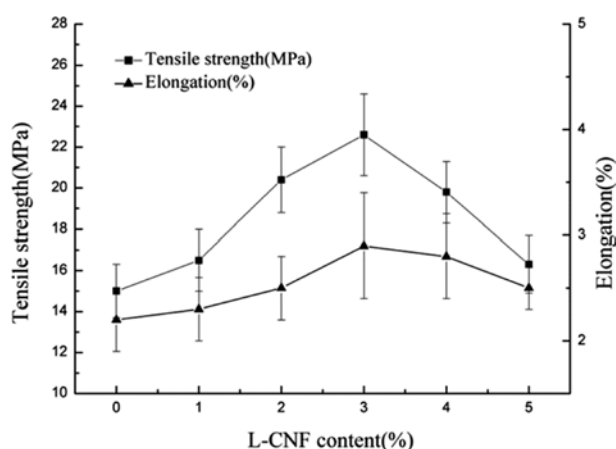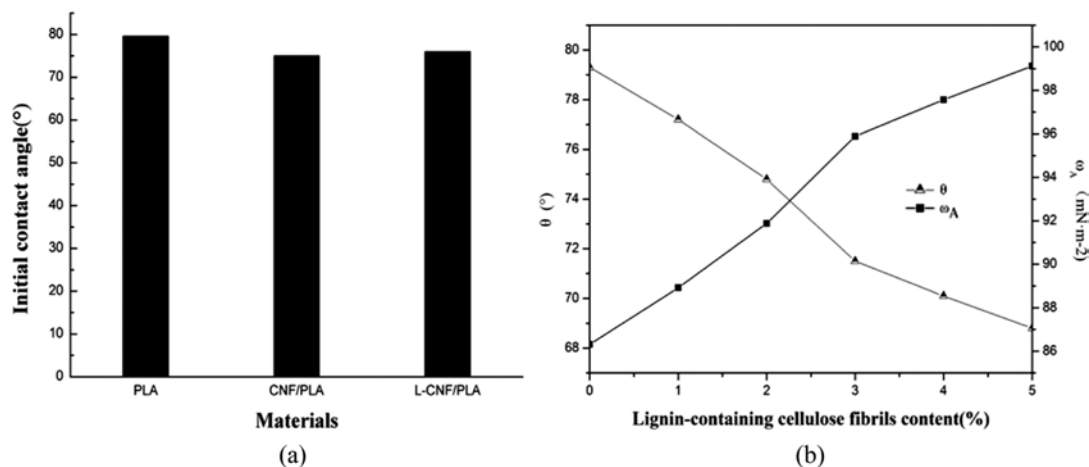
Figure 5. (a) Initial contact angle of three different samples; (b) hydrophilic angle and surface energy of PLA composites with different content of lignin-containing cellulose nanofibrils.

nificantly influence the mechanical strength, The results of contact angle indicated that hydrophilic L-CNF, which contained large amount of hydroxyl groups, were exposed on the PLA composites surface to improve the hydrophilicity property.

Fracture Surfaces of Nanocomposites. SEM photos show the fracture surface morphology of the pure PLA and PLA with different content of L-CNF. Relatively smooth fractures can be seen in Figure 6(a) for the pure PLA.

Under high energy electron beam, the PLA and L-CNF are low in contrast. So the dispersion conditions of L-CNF in PLA matrix can't be seen. The SEM analysis has been used to investigate the fracture mode of the composite and the micrographs have been taken on the tensile fracture surface. From Figure 6(c), the tough characteristics are demonstrated with a rough fracture surface deformed PLA matrix, and upon high magnification (Figure 6(d)), some draw deformation phenomenon was seen. When the content of L-CNF increased to 3.0%, the fracture section become uneven due to the interfacial adhesive force between L-CNF which can be seen from the Figure 6(e, f). Figure 6(f) shows that the presence of aggregation at the surface and fiber breakage. The fiber pull-out in micro-graphs is an indication of low fiber/matrix adhesion. The results show trends similar to those of mechanical properties to the L-CNF/PLA composites, this phenomenon which was also observed by Lee et al.[20] When continue to increase the content of L-CNF to 5%, the fracture structure can be seen from Figure 6(g, h), it did not have the obvious uneven character which can be explained for the increased aggregation among nanofibrils.
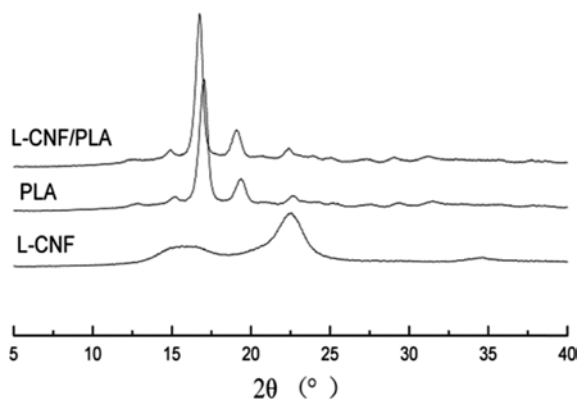
X-Ray Diffraction Study of Nanocomposites. The crys-
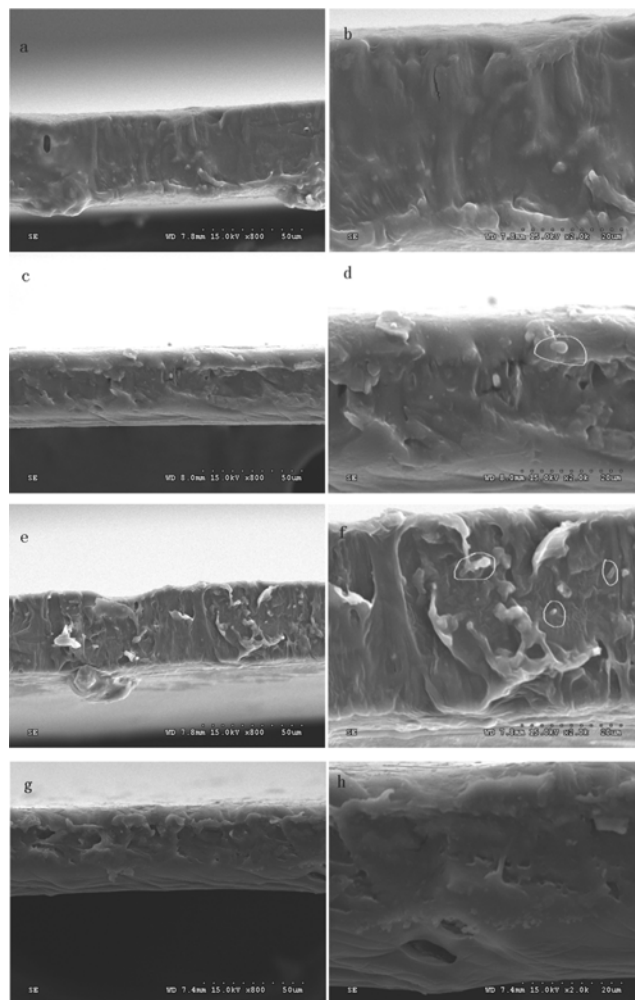
Figure 6. SEM micrographs of fracture surfaces of pure PLA (a, b) and different content of L-CNF of PLA composites: 1% (c, d); 3% (e, f); 5% (g, h).

tallization properties of L-CNF produced and its effect on the PLA nanocomposites of crystallization was investigated using XRD. Figure 7 shows the X-ray diffraction of the L-CNF and the nanocomposite. From the diffraction pattern of L-CNF the highest peak was observed at $2\theta=22.6^{\circ}$ and the double peak signal at $2\theta=14.9^{\circ}$ and 16.5°. The peaks at $2\theta=14.9^{\circ}$, 16.5°, and 22.6° were related to (002) and (001) crystallographic planes, respectively. Both of the two peaks could be attributed to cellulose *I*, which has a monoclinic structure. Lignin was amorphous substance, The crystallinity index of L-CNF was 59%. The main diffraction peaks for PLA alone was seen at $2\theta=16.5^{\circ}$ and 18.9° and a weaker peak at around 22.5° which was also consistent with literature values.[21,22] The diffraction trace for the L-CNF/PLA composite showed clear retention of the L-CNF crystallinity with increasing peaks at $2\theta=14.9^{\circ}$, 16.5, and 22.6°, and this was suggested to be due to an increase in the crystallinity of the L-CNF/PLA composite, according to the XRD pattern, the crystallinity degree of PLA nanocomposites was 31.5% and increased by 2.5% compared to the pure PLA. The difference can be explained by adding L-CNF with high crystallinity degree.

FTIR Characterization of Nanocomposites. The interaction of polymer composites can be identified by using FTIR analysis method. If two polymers blends are completely immiscible, then there are no obvious changes in the FTIR spectra compared with those of each component.[23] If two polymers are compatible, the appreciable chemical interaction occurred between their chains, causing the spectra of composites to change. This results in indentifying segment interaction and providing information about phase behavior of polymer composites. The results indicated the hydrogen bonds existing in the surface of L-CNF and the terminal hydroxyl, terminal carboxyl, and carbonyl groups of PLA.

Figure 8 shows the FTIR spectra of CNF and L-CNF (pure PLA membrane and L-CNF/PLA composite). It can be obtained from the spectra that the hydrogen bonded -OH stretching was located at 3347 cm^{-1}, the C-H stretching at 2903 cm^{-1}, -CH$_2$ bending situates at 1429 cm^{-1}, and the C-H bending at 1370 cm^{-1}, which represent the characteristic peak of cellulose. Lignin spectrum contains a very intense band between 3000 and 2800 cm^{-1} attributed to the C-H stretching from aliphatic chains, and two weak broad band centered at approximately 3400 and 2660 cm^{-1} due to the O-H stretching from hydroxyl and respective carboxyl groups.[24] It can be observed from the spectrum of L-CNF that the peak of 3347 cm^{-1} of CNF has moved to some 3400 cm^{-1}, it could be explained the O-H stretching at 3400 cm^{-1} of lignin made it happen, aromatic ring stretch of lignin gives rise to the 1545 cm^{-1} weak signal.[25]

Figure 9 shows the FTIR spectra of pure PLA membrane, PLA/CNF and L-CNF/PLA composites. The spectra of PLA indicate the characteristic peaks of PLA correspond to the PLA molecular structure.[26,27] The stretching and bending peaks of the C=O appear at 1746 and 1270 cm^{-1} respectively. The peaks at 2999, 2947, 1358, and 1365 cm^{-1} are the asymmetric stretching, symmetric stretching, symmetric bending and asymmetric bending. The C-O stretching was observed at 1192, 1134, and 1096 cm^{-1}.

With the addition of the L-CNF, The peak at 3340 cm^{-1} could be observed wider in L-CNF/PLA, while it couldn't be found in PLA, the C=O peak at 1746 cm^{-1} had a small but definite shift to a higher wavenumber (1751 cm^{-1}) for the main PLA peak, while the C=O peak at 1746 cm^{-1} of PLA/CNF did not shifted to a higher wavenumber. The shift to a lower wavenumber is indicative of hydrogen bonding interactions because

Figure 7. X-Ray diffraction of L-CNF, pure PLA, and L-CNF/PLA composite.
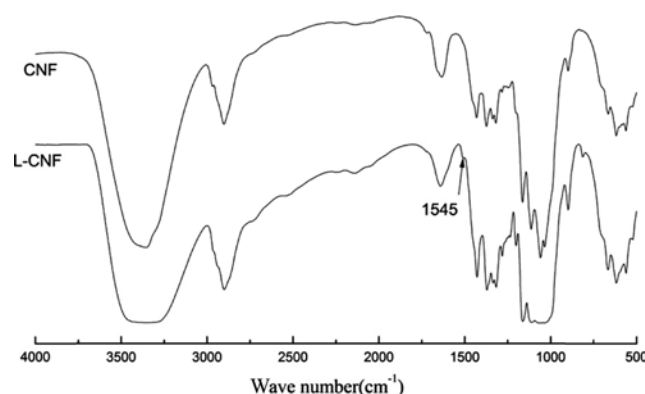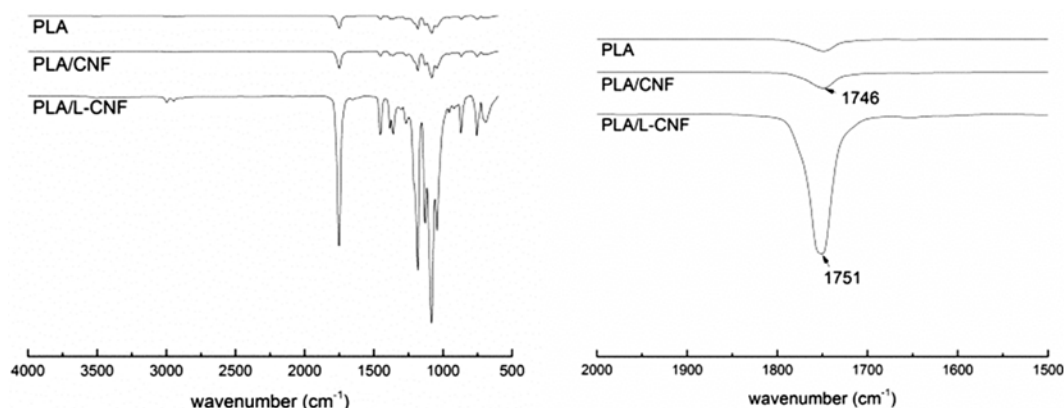

Figure 8. FTIR of CNF and L-CNF.

Figure 9. FTIR of pure PLA, CNF/PLA, and L-CNF/PLA composites.

the stretching frequencies of participating groups usually move toward higher wavenumber.[28] Which indicates that the hydrogen bonds forms between C=O of PLA and the -OH of L-CNF. This indicates that the L-CNF had dispersed in PLA matrix, the L-CNF had a good compatibility with PLA.

Conclusions

Naonocomposites based on the PLA and L-CNF were prepared successfully, a chemo-mechanical method was applied to make the L-CNF disperse in the organic solvent without the freeze-drying process. The mechanical and hydrophilic properties of nanocomposite were increased apparently by adding L-CNF to the PLA matrix. The SEM images indicated that L-CNF could disperse well in PLA matrix. According to the XRD analysis, the degree of crystallinity of PLA nanocomposites was enhanced by adding L-CNF. It also could be seen from the FTIR spectra that the L-CNF had formed hydrogen-bonding or dipolar interactions with PLA. This L-CNF/PLA composite should be widely applied in packaging fields in the further.

References

1. E. Green, E. Stutte, and P. T. C. Harrison, *Sci. Total Environ.*, **256**, 205 (2006).
2. J. H. Yang, J. G. Yu, and Y. Feng, *Carbohydr. Polym.*, **69**, 256 (2006).
3. P. Mangiacapra, G. Gorrasi, and A. Sorrentino, *Carbohydr. Polym.*, **64**, 516 (2005).
4. S. I. Marras and I. Zuburtikudis, *Eur. Polym. J.*, **43**, 2191 (2007).
5. H. Anuar, A. Zuraida, and J. G. Kovacs, *J. Thermoplast. Compos.*, **25**, 153 (2012).
6. R. Mat Taib, Z. A. Ghaleb, and Z. A. Mohd Ishak, *J. Appl. Polym. Sci.*, **123**, 2715 (2012).
7. M. Farhoodi, S. Dadashi, and F. Hemmati, *Polymer(Korea)*, **36**, 745 (2012).
8. C. S. Wu, *Micromol. Biosci.*, **8**, 560 (2008).
9. B. Xiao, X. F. Sun, and R. Sun, *Polym. Degrad. Stab.*, **71**, 223 (2001).
10. L. J. Chun and H. Yong, *Polym. Int.*, **52**, 949 (2003).
11. S. Beck-Candanedo, M. Roman, and D. G. Gray, *Biomacromolecules*, **6**, 1048 (2005).
12. D. Bondeson, A. Mathew, and K. Oksman, *Cellulose*, **13**, 171 (2006).
13. N. Takahashi and K. Okubo, *Bamboo. J.*, **22**, 81 (2005).
14. W. Tao and D. T. Lawrence, *ACS Appl. Mater. Interfaces*, **10**, 1021 (2010).
15. M. N. Angles and A. Dufresne, *Macromolecules*, **34**, 2921 (2001).
16. M. A. Samir, F. Alloin, and J. Y. Sanchez, *Macromolecules*, **37**, 4839 (2004).
17. C. S. Wu and H. T. Liao, *Polymer*, **46**, 10017 (2005).
18. K. S. Kang, B. S. Kim, W. Y. Jang, and B. Y. Shin, *Polymer (Korea)*, **32**, 164 (2009).
19. K. L. Spence, R. A. Venditti, and O. J. Rojas, *Cellulose*, **17**, 835 (2010).
20. S. H. Lee, D. J. Kim, and J. H. Kim, *Polymer(Korea)*, **28**, 519 (2004).
21. K. M. Zakir and C. D. Rudd, *J. Mater. Sci.*, **47**, 2675 (2012).
22. J. H. Lee, Y. H. Lee, and D. S. Lee, *Polymer(Korea)*, **29**, 375 (2005).
23. K. Oksman, A. P. Mathew, and D. Bondeson, *Compos. Sci. Technol.*, **66**, 2776 (2006).
24. J. F. Kadla and S. Kubo, *Composites A*, **35**, 395 (2004).
25. P. Mousaviouna, O. S. William, and G. Georgeb, *Ind. Crop. Prod.*, **32**, 656 (2010).
26. M. Agarwal, K. W. Koelling, and J. J. Chalmers, *Biotechnol. Progr.*, **14**, 517 (1998).
27. T. Miyata and T. Masuko, *Polymer*, **39**, 551 (1998).
28. M. Barsbay and A. Güner, *Carbohydr. Polym.*, **69**, 214 (2007).